Du *et al. Complex Eng Syst* 2024;4:9
DOI: 10.20517/ces.2024.15

Complex Engineering Systems

Research Article

Open Access

A comprehensive risk prediction method for defense mission planning based on probabilistic reasoning and hierarchical analysis

WeiWei Du[1,2], XiaoWei Chen[3,4]

[1]School of Mechanical and Electrical Engineering, Beijing Institute of Technology, Beijin 100081, China.
[2]North Automatic Control Technology Institute, Taiyuan 030006, Shanxi, China.
[3]State Key Laboratory of Explosion Science and Technology, Beijing Institute of Technology, Beijing 100081, China.
[4]Institute of Frontier Interdisciplinary Sciences, Beijing Institute of Technology, Beijing 100081, China.

Correspondence to: Prof. XiaoWei Chen, State Key Laboratory of Explosion Science and Technology, Beijing Institute of Technology, 5 Zhongguancun South Street, Haidian District, Beijing 100081, China. E-mail: chenxiaoweintu@bit.edu.cn

How to cite this article: Du W, Chen X. A comprehensive risk prediction method for defense mission planning based on probabilistic reasoning and hierarchical analysis. *Complex Eng Syst* 2024;4:9. http://dx.doi.org/10.20517/ces.2024.15

Received: 29 Mar 2024 **First Decision:** 9 May 2024 **Revised:** 21 May 2024 **Accepted:** 24 May 2024 **Published:** 31 May 2024

Academic Editor: Hamid Reza Karimi **Copy Editor:** Fangling Lan **Production Editor:** Fangling Lan

Abstract

Most existing risk prediction methods focus on constructing risk element sets and analyzing their uncertainties but do not deeply explore the correlation types and intensities of factors, resulting in large errors in the comprehensive risk prediction results. In this paper, a new integrated risk prediction method is proposed based on the correlation types of tasks in defense task planning and execution. The approach mainly includes the following steps: First, based on the difference of the sequence and mode of action of link tasks, three correlation types (hierarchical, synergistic, and independent) are defined among them, and various correlation measurement techniques are proposed to model these abstract correlation relations and provide data basis for constructing risk decision graphs. Secondly, the rotation extraction strategy is introduced to excavate the internal correlation law between link tasks and generate their hierarchical topology to ensure the rational distribution of their hierarchy positions in defense missions. Then, the intra-layer risk weight is determined based on the centrality of each node in the topology structure, and then the comprehensive risk prediction weighting graph is constructed. Finally, the path analysis is used to assess the rationality of the hierarchical topology structure of the link tasks, and the validity of the proposed method is verified using the test sample set. The results show that compared with other approaches, the predicted results of the proposed method more closely approximate the actual outcomes.

Keywords: Defense mission planning, risk prediction, associative relationships, hierarchical topology, decision mapping

1. INTRODUCTION

Defense task planning[1–3] involves the comprehensive layout and detailed strategizing of specific defense measures by commanders before executing a specific task. This process mainly includes task understanding, analysis and judgment, formulation of concepts, program development, program selection, plan development, and other links. Each stage aims to achieve the overall objective with a clear purpose and specific function. The reasonableness of mission planning and the effectiveness of its execution directly determine the outcome of the entire defense mission. Therefore, risk decision-making for the specific defense mission is a necessary precondition to ensure its successful implementation.

Scholars have achieved certain research results on risk prediction in defense mission planning[4], medical system research and development[5], commercial project risk management[6], and risk assessment of construction projects[7], mainly in the methods of multi-attribute decision-making[8], decision tree analysis[9], and so on. Wu *et al.* analyzed various factors influencing the slope stability, including hydrological conditions of open-pit mines, the geologic formations of slopes, the internal structure[10], *etc.* They identified the attribute sets affecting slope stability and proposed a large-scale multi-attribute group decision-making model based on intuitionistic fuzzy sets. This kind of decision model requires relative independence among the attributes in the set. Decision tree analysis is an analytical method for systematic decision-making after a unified combination arrangement on the premise of classifying the attributes affecting the event; e.g., Ikwan *et al.* constructed a decision tree from the attributes of environmental impacts, management constraints, human/equipment failure factors, and risk factors of the tanks themselves and put forth a fishbone diagram-decision tree-risk matrix analysis strategy, which realized an effective prediction of the effective prediction of tank leakage risk[11]. Zheng *et al.* explored the composition of the mission conception risk assessment system from the levels of thoroughness, mobility, and protection by combining the conception elements and research and judgment data and solved the problem of quantifying the risk of defense conception by establishing the quantitative analysis model of each assessment index[12]. Song *et al.* proposed a program based on the task derivation by establishing a program index system under the background of the joint task risk analysis model[13]. Ryczy□ski *et al.* proposed a risk analysis technique integrating the Kaplan method, the Garrick method, and fuzzy theory to realize the risk management decision-making in the liquid fuel material supply program during military operations[14]. Kim *et al.* introduced the Risk Management Framework (RMF) and developed an assessment model of the weapon system, which offers a theoretical foundation for the mission plan formulation[15]. Most of the above research results focus on constructing risk element sets and analyzing their uncertainty; however, comprehensive prediction is needed on the premise that risk factors are independent.

Subsequently, researchers have made significant efforts in comprehensive risk prediction based on factor associations; e.g., Zhang *et al.*[16] proposed the project portfolio risk (PPR) evolution and response model to solve the problem of project risk interaction, which effectively reflected the real-time interaction in the evolution process of PPRs and helped decision makers quickly identify key strategic intrusion nodes[16]. Zhang *et al.*[16] proposed a category-based association measurement technology (the Measuring Attractiveness by a Categorical-Based Evaluation Technique (MACBETH)) to measure the associative relationships between risks and construct a risk response model for the selection of risk relationships in the medical system research and development project (Risk Response Actions (RRA)), so as to maximize the expectations of the management of medical system research and development project under budget constraints[5] . Abedzadeh *et al.* used fuzzy decision tree analysis to determine the possible combinatorial relationships among social, economic, environmental, and water damage index attributes to achieve an integrated risk management decision for developing

water resources [17]. These methods provide a quantitative assessment of the similarity of risk associations and, to some extent, reveal the linkages and impacts between various risks. In fact, in defense mission planning, not only do the tasks adhere to a strict time sequence, but they also follow layer-by-layer refinement. Directly applying the correlation method mentioned to the defense mission planning for risk prediction will lead to large errors in the prediction results. Hierarchical directed topology lays out the nodes of a complex system according to a hierarchical structure. Inspired by this, hierarchical topology is used in the integrated risk prediction of defense tasks. This technique not only effectively highlights the inter-association relationship among link tasks but also reveals the roles of each task on the defense missions, thereby enhancing the accuracy of the integrated risk prediction.

The main contributions of this paper are as follows: (1) oriented to the task execution process in defense mission planning, the association relationship between tasks in different planning links is studied, and the normalized description of hierarchical, synergistic, and independent relationships and the measurement calculation method are defined; (2) the hierarchical topology between link tasks is generated using the rotational extraction method; (3) on the premise of clarifying the role of each link task on the whole defense mission, a new integrated risk prediction approach is proposed by constructing a weighted map of integrated risk prediction; and (4) combined with specific defense tasks, the proposed method is analyzed qualitatively and quantitatively, and its effectiveness and feasibility are verified.

The structure of this paper is outlined as follows: Section 2 gives the research idea and schematic diagram for constructing a model of the integrated risk prediction problem for defense mission planning; Section 3 defines the three association types and their quantification techniques; Section 4 describes the process of generating the hierarchical topology for link missions; Section 5 proposes a new integrated risk prediction method based on weighted mapping; Section 6 analyzes and validates the proposed approach; Section 7 provides the conclusion.

2. PROBLEM MODELING

To improve the reliability of risk prediction of defense mission planning, this paper, based on the "OODA" (Observe, Orient, Decide, and Act) ring, decomposes the tasks involved into six links and further divides them into four aspects: acquiring information about the defense mission, analyzing the composition of the execution force, evaluating the capability of the attacking entity, and assessing the execution program and plan. The paper specifically examines 15 links of task risk, such as clarifying the defense information, identifying the force of our unit, determining the scale of the attacking entity, and evaluating the resilience of the program. Aimed at the strong temporal sequence of link tasks and their complexity and intertwined relationships, this paper mainly examined the following three aspects: determining their relationships, constructing their hierarchical topology, and developing a comprehensive risk prediction model. The schematic diagram of this prediction model is shown in Figure 1.

The functions of each part are as follows:

(i) As each link follows a strict timing sequence and contains various subtasks, many complex associations may exist between different link tasks. Rationally distinguishing and describing these relationships is the basis for improving the reliability of comprehensive risk prediction. In this paper, we determine the associations by mining the relationship between their time sequences and hierarchies. We specify the association types, give a normalized description of these relationships, and outline the calculation method of the association measures to provide numerical inputs for establishing the probability association matrix between link tasks.

(ii) The relationship between link tasks directly determines the mode and intensity of the role of each link to the total task, and the correlation type varies among various link tasks, which directly affects the comprehensive

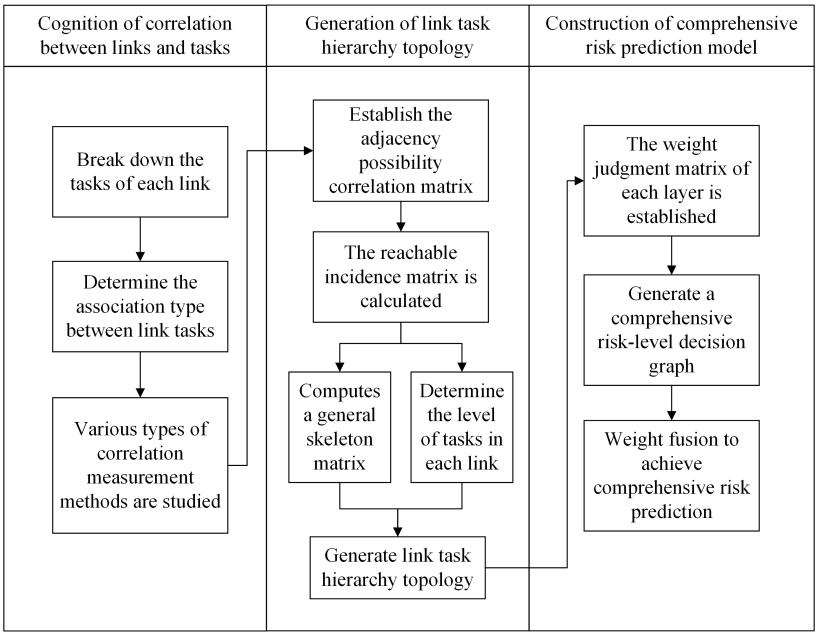

Figure 1. Schematic diagram of the integrated risk prediction model.

risk prediction. The correct construction of link task hierarchical topology is the key to improving the reliability of comprehensive risk prediction. Therefore, this paper clarifies the role and intensity of link tasks on the whole defense task based on the association measurement size of each task in (i), establishes the possibility association matrix, and introduces the rotation extraction method to determine the hierarchical position of the link tasks, which provides a theoretical basis for constructing the comprehensive risk decision-making mapping.

(iii) The risk of each link task acts on the total risk of the defense task based on the topology between link tasks. However, the correlation strength between link tasks is independent, so determining the link task risk weights based on the correlation distribution is a guarantee to enhance the reliability of the comprehensive risk prediction. In this paper, a three-scale hierarchical analysis is conducted based on the centrality of each link task to determine its hierarchical weights, and then a weighted map is constructed to ensure the reliability of the comprehensive risk prediction results.

3. PERCEPTION OF THE CORRELATION BETWEEN LINK TASKS

3.1. Analysis of the correlation between the link tasks

Defense task planning needs to strictly follow the chronological order of the specific measures taken by each link to gradually refine; when a subsequent link task depends on a preceding task, there is a hierarchical relationship between them [18]; when multiple tasks converge into a single task, they share a synergistic relationship; when there is no intrinsic link between the link tasks, they have an independent relationship [19]. The specific description is as follows:

(1) Hierarchical relationship: the correlation between link tasks R_i and R_j is submissive transfer, and R_j needs to depend on the information passed in one direction by R_i to execute, noted as HR.

(2) Synergy relationship: link tasks R_i and R_j act synergistically on link task R_k; then, the correlation between R_i, R_j and R_k is called synergy relationship, and R_k needs to depend on the output information of both R_i and R_j to execute, denoted as SR.

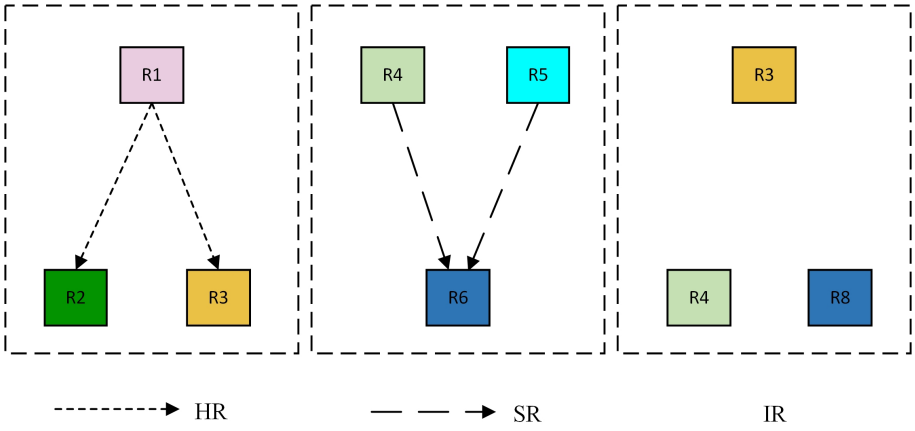

Figure 2. Schematic diagram of the correlation between the link tasks

(3) Independent relationship: there is no interaction of information between link tasks R_i and R_j; there is no dependency between them, and each can execute independently, which is recorded as IR.

In principle, the three types of relationships mentioned are unique: only one type can exist between tasks of the same link. Meanwhile, given the sequential execution of the link tasks and the gradual elaboration of the planning content, all these relationships are unidirectional, from previous to subsequent link tasks.

The schematic diagram of the correlation between the link tasks is depicted in Figure 2. The colors represent the specific link in which each task is located, such as the hierarchical relationship between R_1 and R_2, R_3, the synergistic relationship between R_4, R_5 and R_6, and no obvious relationship between R_3, R_4 and R_8.

3.2. Measurement of the degree of correlation between link tasks

This study uses the degree of association to measure the relationship between link tasks. Subsequently, we determine this degree from the nature of various association relationships.

(1) Calculation of HR relevance

Since the information between the tasks of each link in HR has one-way transferability and the correlation between tasks increases with the similarity of the situational information affecting them, the number of basic situational information inputs to any two link tasks is analyzed using the ensemble similarity measure function [20–22], which measures the HR correlation between the link tasks, expressed as

$$\zeta_{i\to j}^{(\mathrm{HR})} = \frac{2\left\{SI(R_i)\cap SI(R_j)\right\}}{\{SI(R_i)\}+\left\{SI(R_j)\right\}} \tag{1}$$

where $SI(g)$ is the basic situation information input when performing the g-th session task, $\{SI(g)\}$ is the number of situation posture information input when performing the g-th session task, and $\left\{SI(R_i)\cap SI(R_j)\right\}$ denotes the number of intersections of $SI(R_i)$ and $SI(R_j)$.

(2) SR relevance calculation

Unlike HR, SR is more inclined to the joint impact of the execution effect of two or more link tasks on another. Fuzzy hierarchical analysis [23–25] is considered to measure the effect factor of each link task on its acted task,

that is, to calculate the SR correlation between link tasks from a functional perspective.

Assuming that a total of n session tasks have a common effect on R_k when a defense task is planned, the SR correlation between the i-th session task R_i and the k-th session task R_k ($i \in [1, n]$, $k \in [1, n]$ $(k \neq i)$) is

$$\zeta_{i\to k}^{\mathrm{SR}} = \frac{\mathrm{Im}\,(R_i \to R_k)}{\sum_{i=1}^{n} \mathrm{Im}\,(R_i \to R_k)} \tag{2}$$

where $\mathrm{Im}(R_i \to R_k)$ denotes the action factor of the i-th link task R_{i} on R_k, which needs to be inferred using fuzzy hierarchical analysis to derive the extent to which each of the n link tasks acts on R_k.

(3) IR relevance calculation

When the link task R_i is related to R_j as IR, there is no interdependence between these two tasks. Therefore, for any link task, when the relationship between them is IR, then there is $\zeta_{i\to j}^{(\mathrm{IR})} = 0$.

In summary, for a particular defense task, the correlation $\Gamma(R_i, R_j)$ between the link tasks in its planning can be expressed in a triple as follows:

$$\Gamma(R_i, R_j) = \left\langle R_i, \zeta_{i\to j}^{(*)}, R_j \right\rangle \tag{3}$$

where R_i and R_j are the i-th and j-th link tasks, respectively; $\zeta_{i\to j}^{(*)}$ denotes the degree of association, when the association between R_i and R_j is a $*$-relationship, and $* \in \{\mathrm{HR}, \mathrm{SR}, \mathrm{IR}\}$, $\zeta_{i\to j}^{(*)} \in [0, 1]$.

4. LINK TASK HIERARCHY TOPOLOGY GENERATION

4.1. Adjacency probability correlation matrix

Assuming that a total of n link tasks are involved in planning a specific defense task, for two link tasks R_i and R_j, since HR, SR, and IR are unique, the correlation between them can be expressed as

$$\zeta_{i\to j} = \zeta_{i\to j}^{(\mathrm{HR})} \quad or \quad \zeta_{i\to j}^{(\mathrm{SR})} \quad or \quad \zeta_{i\to j}^{(\mathrm{IR})} \tag{4}$$

In addition, due to the temporal nature of the adjacent links in planning, for the convenience of the subsequent study, the link tasks are sorted in strict time order of execution. Thus, the adjacency correlation matrix between the link tasks is established based on the values of the degree of correlation between them. Considering that the degree of correlation takes values between 0 and 1, instead of only 0 and 1, we distinguish it from the traditional adjacency correlation matrix, which is called the adjacency possibility correlation matrix $\Gamma_{n\times n}$ here.

$$\Gamma_{n\times n} = \left(\zeta_{i\to j}\right)_{n\times n} = \begin{bmatrix} 0 & \cdots & \cdots & \zeta_{1\to j} & \cdots & \zeta_{1\to n} \\ 0 & 0 & \cdots & \cdots & \cdots & \cdots \\ 0 & 0 & 0 & \zeta_{i\to j} & \cdots & \zeta_{i\to n} \\ 0 & 0 & 0 & 0 & \cdots & \cdots \\ 0 & 0 & 0 & 0 & 0 & \cdots \\ 0 & 0 & 0 & 0 & 0 & 0 \end{bmatrix} \tag{5}$$

Since the adjacency possibility association matrix $\Gamma_{n\times n}$ emphasizes the unidirectional association between different link tasks and does not consider the own association of the link task, Equation (5) is a triangular array with diagonal elements of zero.

4.2. Calculation of the possibility hierarchy position for the link tasks

To ensure that the link tasks directly related to the total task are classified in the innermost layer, while the fundamental link tasks that affect the total task are classified in the outermost layer, the concept of rotational extraction [26] is used to calculate the possibility hierarchy position of each link task in the total task [27,28]; that is, the innermost and outermost layers are determined first. Subsequently, the next inner and outer layers are followed by the next-sub-inner and -outer layers until all link tasks are assigned. The implementation process is as follows:

(i) Combining the unit matrix I, the adjacency possibility correlation matrix $\Gamma_{n\times n}$ is concatenated until the matrix does not change to obtain the reachable correlation matrix $M_{n\times n}^{i\to j}$:

$$M_{n\times n}^{i\to j} = \left(\left(\zeta_{i\to j}\right)_{n\times n} + (I)_{n\times n}\right)^{k+1} = \left(\left(\zeta_{i\to j}\right)_{n\times n} + (I)_{n\times n}\right)^{k} \neq \left(\left(\zeta_{i\to j}\right)_{n\times n} + (I)_{n\times n}\right)^{k-1} \tag{6}$$

(ii) The link tasks in each column and row corresponding to all elements in row t and column t of $M_{n\times n}^{i\to j}$ that are not zero are noted as the sets $A(R_t)$ and $B(R_t)$, respectively. Let the intersection of the two sets be $C(R_t)$. Subsequently, the link tasks in the innermost and outermost layers are determined according to the following rules.

$$\begin{cases} \text{Divide the extracted session tasks to the innermost layer when } C\left(R_t\right) = A\left(R_t\right) \bigcap B\left(R_t\right) = A\left(R_t\right) \\ \text{Divide the extracted session tasks to the outermost layer when } C\left(R_t\right) = A\left(R_t\right) \bigcap B\left(R_t\right) = B\left(R_t\right) \end{cases} \tag{7}$$

(iii) The link tasks set as the innermost and outermost layers in Step (2) are removed from the reachable association matrix $M_{n\times n}^{i\to j}$. If m link task items are removed at this point, a reachable association matrix $M_{(n-m)\times(n-m)}^{i\to j(1)}$ of order $n-m$ is obtained, and Step (2) is repeated to determine the link tasks located in the next inner and outer layers.

(iv) The sub-inner and sub-outer link tasks identified in Step (3) are removed from the reachable association matrix $M_{(n-m)\times(n-m)}^{i\to j(1)}$. If c link task items are removed at this point, a reachable association matrix $M_{(n-m-c)\times(n-m-c)}^{i\to j(2)}$ of order $n-m-c$ is obtained, and Step (2) is repeated to identify the link tasks located in the sub-inner and sub-outer layers until all link task items have been set.

(v) The following operations are performed on the reachable correlation matrix $M_{n\times n}^{i\to j}$ to create a general skeleton matrix $E_{n\times n}$:

$$E_{n\times n}=\left(e_{ij}\right)_{n\times n} = M_{n\times n}^{i\to j} - \left(M_{n\times n}^{i\to j} - (I)_{n\times n}\right)^2 - (I)_{n\times n} \tag{8}$$

The position of the possibility hierarchy for each link task is determined based on Step (4).

5. INTEGRATED RISK PREDICTION MODELING

5.1. Calculation of task risk weights and integrated risk

The process of realization is as follows:

(i) With the link task risk as the sub-node and the total task risk as the root node, the link task level position determined in Section 4 is taken as the position of each sub-node relative to the root node, and the hierarchical decision graph of the comprehensive risk is preliminarily determined. Determine the total number of layers K. If the $h \in [1, K]$ layer contains g_{hv} child nodes, calculate the centrality of each child node according to the general skeleton matrix $E_{n\times n}$ as follows:

$$C(F_t) = \sum_{j=1}^{n} e_{tj} + \sum_{i=1}^{n} e_{it} \tag{9}$$

where F_t is the tth child node, e_{tj} is the degree of association between the tth child node and the j $(j = 1, 2, \cdots, n)$th child node, and e_{it} is the degree of association between the ith child node and the tth child node.

The child node centrality at layer h is compared pairwise and assigned on a three-scale degree:

$$b_{lk} = \begin{cases} 2 & C(F_l) > C(F_k) \\ 1 & C(F_l) = C(F_k) \\ 0 & C(F_l) < C(F_k) \end{cases}, l, k = 1, 2, ..., g_{hv} \tag{10}$$

Then, the weight judgment matrix of the hth layer sub-node is built.

$$B_h = \begin{bmatrix} b_{11} & \cdots & b_{1j} & \cdots & b_{1g_{hv}} \\ \cdots & \cdots & \cdots & \cdots & \cdots \\ b_{i1} & \cdots & b_{ij} & \cdots & b_{ig_{hv}} \\ \cdots & \cdots & \cdots & \cdots & \cdots \\ b_{g_{hv}1} & \cdots & b_{g_{hv}j} & \cdots & b_{g_{hv}g_{hv}} \end{bmatrix} \tag{11}$$

(ii) According to the weight judgment matrix B_h, the proposed optimal transfer matrix[29] $U_h=(u_{lk})_{g_{hv}\times g_{hv}}$ is established, and the element u_{lk} is determined using

$$u_{lk} = \exp\left(\frac{1}{g_{hv}} \sum_{q=1}^{g_{hv}} (b_{lq} - b_{kq})\right) \tag{12}$$

The maximum eigenvalue $\lambda_{\max}$ of U_h is calculated and its corresponding eigenvector $\xi_h=(\xi_{h1}, \xi_{h2}, ..., \xi_{hg_{hv}})$ is obtained and normalized to obtain the intra-layer weight vector of the $g_h$sub-nodes of the hth layer, as expressed below:

$$\xi_h{'}=(\xi_{hg_{h1}}{'}, \cdots \xi_{hg_{h2}}{'}, ..., \xi_{hg_{hv}}{'}) \tag{13}$$

where $\xi_{hg_{hr}}{'}$ denotes the intra-layer weight coefficient of the $r \in [1, v]$th child node in the h-th layer. The intra-layer risk weight of each link is used as the connection edge strength between the child nodes to represent

the degree of influence of the previous on the subsequent child nodes. In this way, the weighted graph of comprehensive risk prediction is generated.

(iii) Combining the weight vectors of the child nodes within all the layers, the weight of the impact of each link's risk on the total risk is determined from the top level downwards, and the combined weight of the r-th child node in the h-th layer in the root node is calculated by

$$\omega_{g_{hr}} = \frac{\xi_{hg_{hr}}'}{\sum_{h=1}^{K}\sum_{r=1}^{g_{hv}} \xi_{hg_{h1}}'+\xi_{hg_{h2}}'+\ldots+\xi_{hg_{hr}}'} \tag{14}$$

(iv) The weighted fusion of task risks for each segment yields a combined risk prediction of

$$F = \sum\nolimits_{h=1}^{K} \sum\nolimits_{r=1}^{g_{hv}} F_{hg_{hr}} \times \omega_{g_{hr}} \tag{15}$$

where $F_{hg_{hr}}$ represents the value at risk corresponding to the tasks in each session.

5.2. Comprehensive risk prediction based on weighted mapping

The pseudo-code of the integrated risk prediction model based on weighted mapping is shown in Table 1.

6. CASE VERIFICATION AND COMPARATIVE ANALYSIS

To verify the feasibility and superiority of the proposed method, this section presents an example of defense mission planning.

Assuming that an attacking entity is expected to strike our T-area at a certain time, the commanders plan defense tasks with the acquired basic situational information. A total of 15 tasks within six planning segments are involved in this planning process. The values of risk incurred by the link tasks are shown in Table 2.

6.1. Calculation of the correlation between the link tasks

Here, the reasonableness of resource coordination R_9 is used as an example to illustrate the calculation of its correlation with the others of the tasks. To formulate resource coordination rationality, it is necessary to combine the indicators expected to be achieved by the overall defense task, such as the coverage of the defense area and destruction requirements. The rationality of task indicator setting R_7 is a specific description of the indicators expected to be achieved by the task. Thus, the relationship between R_9 and R_7 belongs to a hierarchy. When combining the basic situational information involved in R_7 and R_9, and their intersection [Table 3], the hierarchical correlation between R_7 and R_9 can be calculated as $\zeta_{7\to9}^{(\mathrm{HR})} = 0.769$ using Equation (1).

Table 1. Integrated risk prediction model pseudo-code

		Integrated risk prediction model pseudo-code
Perceived linkages between session tasks	Step 1	Determine the types of interlinked relationships between link tasks based on the concepts of hierarchical, synergistic and independent relationships.
	Step 2	Using Equations (1) and (2) to calculate the link inter-task correlation, respectively.
Hierarchical topology generation	Step 3	Using Equations (5) and (6) to obtain the adjacency likelihood correlation matrix and the reachability correlation matrix, respectively.
	Step 4	Use Equation (7) to determine the hierarchical position of the tasks in each session.
	Step 5	The general skeleton matrix is computed using Equation (8) and the hierarchical topology is generated.
Consolidated risk projections	Step 6	Using Equations (9-11) to construct the weight judgment matrix of task risk for each layer of the link B_h.
	Step 7	Calculate the weighting coefficients of each segment's task risk in the composite risk using Equations (12-14) to construct a composite risk decision weighting map.
	Step 8	The combined risk is predicted using Equation (15).

Table 2. Information about the session tasks and their corresponding risk items in a given scenario

Session task	Corresponding risk items	Risk value
Defensive message clarity R_1	Unclear defensive information F_1	0.658
Comprehensive information on the attacking entity R_2	Incomplete information about the attacking entity F_2	0.790
Our defense unit strength determination R_3	Our defense unit strength was incorrectly determined F_3	0.566
Judgment of the direction of movement of the attacking entity R_4	Inaccurate judgment of the direction of movement of the attacking entity F_4	0.778
Attack entity size determination R_5	The size of the attacking entity was incorrectly identified F_5	0.721
Unit platform response capability R_6	Inadequate response capability of the unitary platform F_6	0.618
Reasonable setting of task indicators R_7	Unreasonable setting of task indicators F_7	0.692
Reasonableness of the selection of the target of fire collection R_8	Unreasonable selection of fire target F_8	0.764
Rationalization of resource integration R_9	Unreasonable resource integration F_9	0.625
Protective capability in conception R_{10}	Insufficient conceptual protection F_{10}	0.750
Reasonableness of programming standards R_{11}	Unreasonable standards for program development F_{11}	0.615
Program Resilience R_{12}	Inadequate program resilience F_{12}	0.632
Reasonableness of the index system of program preference R_{13}	The index system of program preference is not reasonable F_{13}	0.625
Execution of branch plans R_{14}	Inadequate execution of branch plans F_{14}	0.724
Monitoring capabilities of the program R_{15}	Insufficient monitoring power of the plan F_{15}	0.625

Table 3. Basic situation information related to R_7 and R_9

Serial number	$SI(R_7)$	$SI(R_9)$	$SI(R_7) \cap SI(R_9)$
1	Expected means of mission defense	Expected means of mission defense	1
2	Expected Achievement Goals	Expected Achievement Goals	1
3	Destruction parameter requirements	Destruction parameter requirements	1
4	Coverage	Coverage	1
5	Duration of mission	Duration of mission	1
6	The capability of reconnaissance and early warning unit capability	The capability of reconnaissance and early warning unit capability	1
7	The capability of firepower unit capability	The capability of firepower unit capability	1
8	The capability of electronic countermeasures unit capability	The capability of electronic countermeasures unit capability	1
9	The capability of integrated assurance unit	The capability of integrated assurance unit	1
10	The capability of interceptor strike unit capability	The capability of interceptor strike unit capability	1
11	–	Attack entity equipment type	0
12	–	Number of attacking entity equipment	0
13	–	Attack entity incoming main direction	0
14	–	Attack entity incoming sub-direction	0
15	–	Attack entity incoming proximity direction	0
16	–	Attack entity incoming intent	0

In addition to the hierarchical relationship between R_9 and R_7, R_9 also has a synergistic relationship with defense information clarity R_1, our defense unit strength determination R_3, and attack entity size determination

R_5. For example, when planning a mission, if we ignore the determination of the strength of the specific unit defense measures available to us and the overall determination of the size of the attacking entity of the opponent and directly conceptualize the unit strength, the allocation of unit strength resources will likely be unreasonable and even cause the deployment to fail. In other words, the clarity of defense information, the determination of our defense unit forces, and the determination of the size of the attacking entity all affect the rationality of resource coordination in the conceptualization process, which, together, determine the rationality of our resource coordination. Therefore, a synergistic relationship exists between them and the reasonableness of our resource integration.

To measure the degree of synergy between link tasks, ten experts in related fields determined the role factors of link tasks R_1, R_3 and R_5 on R_9 using fuzzy hierarchical analysis, the fuzzy complementary judgment matrix is as follows:

$$\begin{pmatrix} 0.5 & 0.55 & 0.15 \\ 0.45 & 0.5 & 0.1 \\ 0.85 & 0.9 & 0.5 \end{pmatrix}\begin{pmatrix} 0.5 & 0.5 & 0.2 \\ 0.5 & 0.5 & 0.1 \\ 0.8 & 0.9 & 0.5 \end{pmatrix}\begin{pmatrix} 0.5 & 0.6 & 0.15 \\ 0.4 & 0.5 & 0.05 \\ 0.85 & 0.95 & 0.5 \end{pmatrix}\begin{pmatrix} 0.5 & 0.5 & 0.2 \\ 0.5 & 0.5 & 0.2 \\ 0.8 & 0.8 & 0.5 \end{pmatrix}\begin{pmatrix} 0.5 & 0.6 & 0.1 \\ 0.4 & 0.5 & 0.15 \\ 0.9 & 0.85 & 0.5 \end{pmatrix}$$

$$\begin{pmatrix} 0.5 & 0.55 & 0.15 \\ 0.45 & 0.5 & 0.2 \\ 0.85 & 0.8 & 0.5 \end{pmatrix}\begin{pmatrix} 0.5 & 0.5 & 0.1 \\ 0.5 & 0.5 & 0.05 \\ 0.9 & 0.95 & 0.5 \end{pmatrix}\begin{pmatrix} 0.5 & 0.55 & 0.2 \\ 0.45 & 0.5 & 0.1 \\ 0.8 & 0.9 & 0.5 \end{pmatrix}\begin{pmatrix} 0.5 & 0.6 & 0.15 \\ 0.4 & 0.5 & 0.2 \\ 0.85 & 0.8 & 0.5 \end{pmatrix}\begin{pmatrix} 0.5 & 0.55 & 0.2 \\ 0.45 & 0.5 & 0.05 \\ 0.8 & 0.95 & 0.5 \end{pmatrix}$$

Calculating the action factors of the link tasks R_1, R_3 and R_5 on R_9 based on the above matrix, as shown in Table 4. Based on Table 4, the degrees of correlation between R_1, R_3, R_5 and R_9 were calculated using Equation (2) to obtain $\zeta_{1\to9}^{(SR)} = 0.283$, $\zeta_{3\to9}^{(SR)} = 0.258$, and $\zeta_{5\to9}^{(SR)} = 0.459$.

Since program resilience is not associated with other link tasks, it is considered an independent relationship and acts directly on the total task. The degrees of synergy between all tasks can be calculated based on the analysis of the remaining tasks, which will not be repeated here owing to length constraints. Thus, the adjacency probability correlation matrix $\Gamma_{15\times15}$ [30,31] between the 15 link tasks can be generated, as shown in Table 5:

Where data followed by "*" indicates that the type of relationship between tasks in the session is hierarchical; data followed by "/" denotes that the relationship type between tasks in the session is synergistic.

In turn, the reachable correlation matrix $M_{15\times15}^{i\to j}$ [32–34] and the general skeleton matrix $(E)_{15\times15}$ can be determined, as provided in Tables 6 and 7, respectively:

Therefore, according to the results of link task relevance calculation, the link task relevance structure model can be obtained, as given in Figure 3.

This paper adopts the path analysis method to test the accuracy and reliability of the link task association structure model. Several domain experts are invited to assess the risk value of each link task and use it as a basis for judgment, and the risk value of the corresponding risk item of each link task is imported into the path analysis model for analysis to verify the validity of the association path between each task and the total task [35–37], where the standardized coefficient specifically reflects the degree of influence between the two risks; when the p-value is $< 5\%$, it can be considered significant, representing a valid path between the risks. The specific results are shown in Table 8.

From the results of Table 8, it can be seen that the p-value of paths $R_1 \to R_9$, $R_3 \to R_9$, $R_{12} \to R$ is less than 5%, and that of the rest of the paths is less than 1%, which indicates that the paths existing between risks in the

Table 4. The action factors of the link tasks R_1, R_3 and R_5 on R_9 obtained from FAHP

	$\mathrm{Im}(R_1 \to R_9)$	$\mathrm{Im}(R_3 \to R_9)$	$\mathrm{Im}(R_5 \to R_9)$
Action factor	0.283	0.258	0.459

Table 5. The adjacency probability correlation matrix

$\Gamma_{15\times15} = (\zeta_{i\to j})_{15\times15}$	R_1	R_2	R_3	R_4	R_5	R_6	R_7	R_8	R_9	R_{10}	R_{11}	R_{12}	R_{13}	R_{14}	R_{15}
R_1	0	0	0	0	0	0	0.275/	0	0.283/	0	0	0	0.4*	0	0
R_2	0	0	0.75*	0.462*	0	0	0.6/	0	0	0	0	0	0	0	0
R_3	0	0	0	0	0	0.913*	0.125/	0	0.258/	0	0	0	0	0	0
R_4	0	0	0	0	0	0	0	0.7/	0	0	0	0	0	0	0
R_5	0	0	0	0	0	0	0	0.3/	0.459/	0	0	0	0	0	0
R_6	0	0	0	0	0	0	0	0	0	0.606*	0	0	0	0.92*	0.467*
R_7	0	0	0	0	0	0	0	0	0.769*	0	0	0	0.324*	0	0
R_8	0	0	0	0	0	0	0	0	0	0	0	0	0	0	0
R_9	0	0	0	0	0	0	0	0	0	0	0.64*	0	0	0	0
R_{10}	0	0	0	0	0	0	0	0	0	0	0	0	0	0.541*	0
R_{11}	0	0	0	0	0	0	0	0	0	0	0	0	0	0	0
R_{12}	0	0	0	0	0	0	0	0	0	0	0	0	0	0	0
R_{13}	0	0	0	0	0	0	0	0	0	0	0	0	0	0	0
R_{14}	0	0	0	0	0	0	0	0	0	0	0	0	0	0	0
R_{15}	0	0	0	0	0	0	0	0	0	0	0	0	0	0	0

Table 6. The reachable correlation matrix

$M_{15\times15}^{i\to j}$	R_1	R_2	R_3	R_4	R_5	R_6	R_7	R_8	R_9	R_{10}	R_{11}	R_{12}	R_{13}	R_{14}	R_{15}
R_1	1	0	0	0	0	0	0.275	0	0.283	0	0.283	0	0.4	0	0
R_2	0	1	0	0.75	0.462	0	0.6	0.7	0.6	0	0.6	0	0.324	0	0
R_3	0	0	1	0	0	0.913	0.125	0	0.258	0.606	0.258	0	0.125	0.913	0.467
R_4	0	0	0	1	0	0	0	0.7	0	0	0	0	0	0	0
R_5	0	0	0	0	1	0	0	0.3	0.459	0	0.459	0	0	0	0
R_6	0	0	0	0	0	1	0	0	0	0.606	0	0	0	0.92	0.467
R_7	0	0	0	0	0	0	1	0	0.769	0	0.64	0	0.324	0	0
R_8	0	0	0	0	0	0	0	1	0	0	0	0	0	0	0
R_9	0	0	0	0	0	0	0	0	1	0	0.64	0	0	0	0
R_{10}	0	0	0	0	0	0	0	0	0	1	0	0	0	0.541	0
R_{11}	0	0	0	0	0	0	0	0	0	0	1	0	0	0	0
R_{12}	0	0	0	0	0	0	0	0	0	0	0	1	0	0	0
R_{13}	0	0	0	0	0	0	0	0	0	0	0	0	1	0	0
R_{14}	0	0	0	0	0	0	0	0	0	0	0	0	0	1	0
R_{15}	0	0	0	0	0	0	0	0	0	0	0	0	0	0	1

link task association structure model are effective. And the degree of influence between risks can be reflected by the standardized coefficient value; the larger the standardized coefficient value is, the higher the degree of validity of the existence of paths between risks; according to the results of Table 8, it can be seen that each path distance presents a significant positive correlation (standardized coefficient > 0). Thus, the reliability of the link task association structure model paths is verified.

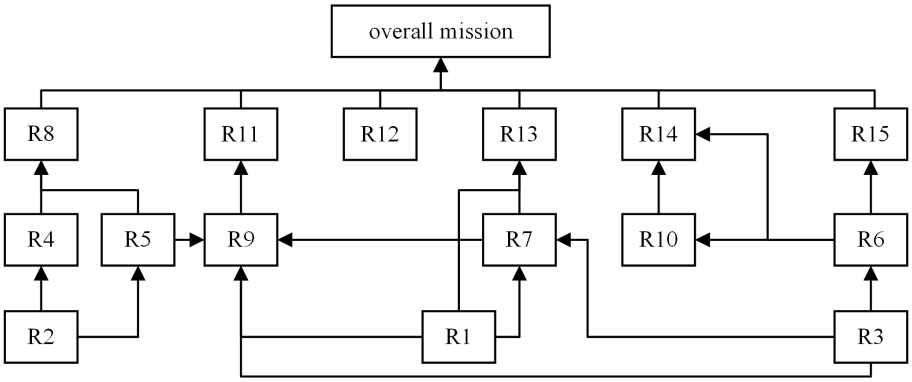

Figure 3. Structural modeling of link task associations

Table 7. The general skeleton matrix

$(E)_{15\times15}$	R_1	R_2	R_3	R_4	R_5	R_6	R_7	R_8	R_9	R_{10}	R_{11}	R_{12}	R_{13}	R_{14}	R_{15}
R_1	0	0	0	0	0	0	0.275	0	0.008	0	0	0	0.125	0	0
R_2	0	0	0	0.75	0.462	0	0.6	0	0	0	0	0	0	0	0
R_3	0	0	0	0	0	0.913	0.125	0	0.133	0	0	0	0	0	0
R_4	0	0	0	0	0	0	0	0.7	0	0	0	0	0	0	0
R_5	0	0	0	0	0	0	0	0.3	0.459	0	0	0	0	0	0
R_6	0	0	0	0	0	0	0	0	0	0.606	0	0	0	0.379	0.467
R_7	0	0	0	0	0	0	0	0	0.769	0	0	0	0.324	0	0
R_8	0	0	0	0	0	0	0	0	0	0	0	0	0	0	0
R_9	0	0	0	0	0	0	0	0	0	0	0.64	0	0	0	0
R_{10}	0	0	0	0	0	0	0	0	0	0	0	0	0	0.541	0
R_{11}	0	0	0	0	0	0	0	0	0	0	0	0	0	0	0
R_{12}	0	0	0	0	0	0	0	0	0	0	0	0	0	0	0
R_{13}	0	0	0	0	0	0	0	0	0	0	0	0	0	0	0
R_{14}	0	0	0	0	0	0	0	0	0	0	0	0	0	0	0
R_{15}	0	0	0	0	0	0	0	0	0	0	0	0	0	0	0

Table 8. Regression coefficients for structural modeling of link task associations

Path	Standardized coefficient	P	Path	Standardized coefficient	P
$R_2 \to R_4$	0.961	<1% (0.000***)	$R_9 \to R_{11}$	0.983	<1% (0.000***)
$R_2 \to R_5$	0.953	<1% (0.000***)	$R_1 \to R_{13}$	0.147	<5% (0.042**)
$R_3 \to R_6$	0.963	<1% (0.000***)	$R_7 \to R_{13}$	0.843	<1% (0.000***)
$R_1 \to R_7$	0.447	<1% (0.000***)	$R_6 \to R_{14}$	0.499	<1% (0.001***)
$R_3 \to R_7$	0.547	<1% (0.000***)	$R_{10} \to R_{14}$	0.495	<1% (0.01***)
$R_4 \to R_8$	0.515	<1% (0.000***)	$R_6 \to R_{15}$	0.974	<1% (0.000***)
$R_5 \to R_8$	0.479	<1% (0.000***)	$R_8 \to R$	0.154	<1% (0.000***)
$R_1 \to R_9$	0.201	<5% (0.029**)	$R_{11} \to R$	0.269	<1% (0.000***)
$R_3 \to R_9$	0.229	<5% (0.023**)	$R_{12} \to R$	0.081	<5% (0.025**)
$R_5 \to R_9$	0.181	<1% (0.07***)	$R_{13} \to R$	0.127	<1% (0.07***)
$R_7 \to R_9$	0.430	<1% (0.01***)	$R_{14} \to R$	0.251	<1% (0.000***)
$R_6 \to R_{10}$	0.976	<1% (0.000***)	$R_{15} \to R$	0.190	<1% (0.01***)

6.2. Risk hierarchy decision weighting mapping construction

Based on the general skeleton matrix $(E)_{15\times15}$, the rotational extraction concept described in Section 4 is used to determine the possibility hierarchy position of the link task in the total task and then generate a risk hierarchy decision weighting mapping $G \updownarrow$ for defense task planning, as shown in Figure 4A. It can be observed from Figure 4A that F_8, F_{11}, F_{12}, F_{13}, F_{14}, and F_{15} act directly on the total risk F, while $F_1 \sim F_7$ and $F_9 \sim F_{10}$ need to act indirectly on F through other intermediate nodes.

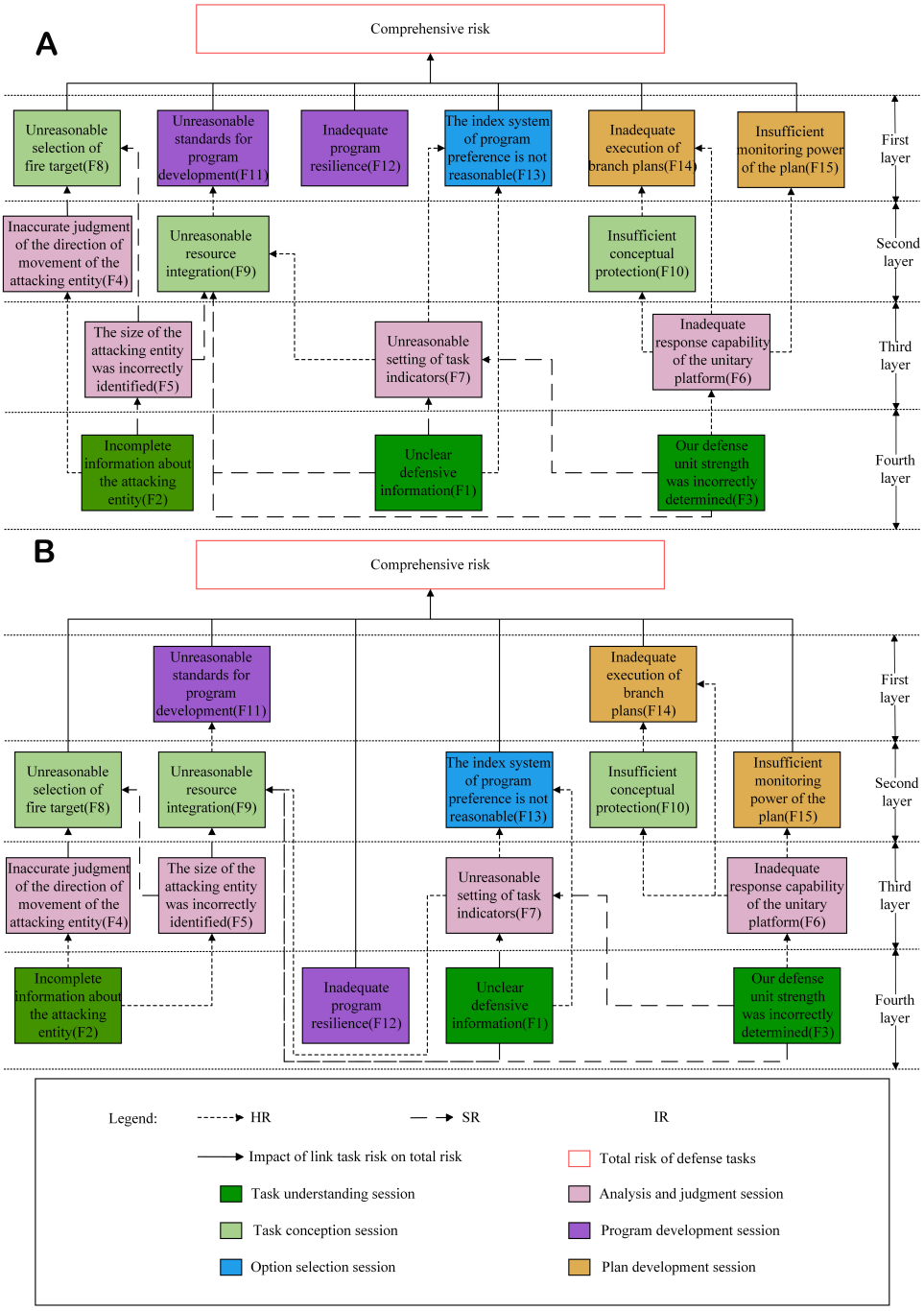

Figure 4. Decision mapping generated by the two methods. (A) Decision mapping of the possibility hierarchy determined by the rotattional extractional method; (B) Decision mapping of the possibility hierarchy determined by bottom-upextractional method.

To illustrate that the generated risk hierarchy decision weighting mapping $G\updownarrow$ is more conducive to the prediction of integrated risks, the rationality of the approach in this study is analyzed by comparing it with the risk hierarchy decision weighting mapping $G\uparrow$[38,39] (shown in Figure 4B) constructed based on the bottom-up explanatory structure model[40].

By comparing Figure 4A and B, we can find that in the $G\uparrow$ generated based on the bottom-up explanation structure model, F_8, F_{12}, F_{13}, and F_{15}, which play a direct role in the total risk, are not assigned to the first layer,

which is closer to the total risk; however, F_8, F_{13}, and F_{15} are assigned to the second and F_{12} is assigned to the forth layer. Moreover, F_4 is influenced by the position of the F_8 layer and is assigned to the third layer that is further away from the total risk. To a certain extent, the direct influence of F_4, F_8, F_{12}, F_{13}, and F_{15} on the total task is weakened, making the corresponding risks of each link task relatively more diffuse in the decision, thereby making it difficult for the decision weighting mapping to be clustered to the total risk. In contrast, $G\updownarrow$ generated by the proposed method, F_8 and $F_{11} \sim F_{15}$, which play a direct role in the total task, are both assigned to the first layer nearest to the total risk. F_4 is assigned to the second layer which is relatively far from the total risk, because it indirectly acts on F through a node F_8. The proposed method is more conducive to clustering each link task to the total task.

To visualize the aforementioned phenomenon, firstly, according to the general skeleton matrix $(E)_{15\times15}$ obtained in Section 5.1, the elements in each nonzero row and column are summed up to obtain the impact value $\sum_{i=1}^{15} e_{ij}$ of other tasks on the ith link task and the impact value $\sum_{j=1}^{15} e_{ij}$ of the ith link task on other tasks. Subsequently, the impact values of each link task are processed in combination with its different levels N ($N = 1, 2, 3, 4$) as follows:

$$\begin{cases} \sum_{i=1}^{15} e_{ij} + (N-1) & \text{The impact value of the other tasks on the } i\text{th link task} \\ \sum_{j=1}^{15} e_{ij} + (N-1) & \text{The impact value of the } i\text{th link task on other tasks} \end{cases} \tag{16}$$

Taking $\sum_{i=1}^{15} e_{ij} + (N-1)$ and $\sum_{j=1}^{15} e_{ij} + (N-1)$ as the horizontal and vertical coordinates of the ith link task, respectively, the possibility hierarchy position distribution of each link task of $F_1 \sim F_{15}$ can be calculated, as shown in Figure 5. Among them,"0, 1, 2, 3, 4" on the coordinate axis represent the boundaries of the four layer task hierarchy established in the defense task planning process, and their physical meaning is the number of hierarchical levels.

It can be intuitively observed from Figure 5 that in the hierarchical decision map $G\updownarrow$ generated by our proposed method, the link tasks are more aggregated to the root node F. In contrast, the link tasks in the method in the literature[40], are more inclined to spread to the branch nodes, which weakens the comprehensive effect on the risk to a certain extent. Therefore, it is more reasonable and feasible to use the decision mapping generated by the proposed method for subsequent integrated risk prediction.

6.3. Forecasting methodology for integrated risk

Based on the general skeleton matrix $(E)_{15\times15}$ and the integrated risk hierarchical decision weighting mapping generated in Section 5.1, the centrality of the link task risk is calculated using Equation (9) (as shown in Table 9), and the numerical comparison is used to establish the link task risk weight judgment matrix $B_h = \left(b_{ij}\right)_{g_h\times g_h}$ for the hth layer, where $h = 1, 2, 3, 4$. Then, Equations (11-14) are used to determine the intra-layer weight and comprehensive weight of the task risk of each layer in the total task risk.

To illustrate the rationality of the above weight determination method, the weights obtained from the bottom-up extraction method[40] and entropy method[41] are compared for analysis, respectively, as shown in Table 10.

Compared to the bottom-up extraction method, the weight values of F_1, F_2, and F_3 in F obtained by the proposed method are higher, which is in line with the needs of defense task planning. The main reason is that the link tasks F_1, F_2, and F_3 are all basic situational information. Only by fully grasping them can the emergence of risks in the execution of the later link tasks be avoided and the completion of the total task be ensured. The risks corresponding to F_8, F_{13}, and F_{15} are raised from the second to the first level in the proposed method, and the weight values are increased because they act directly on F. Simultaneously, the risk corresponding to F_4 increases from the third to the second level, and the weight value is also improved. The

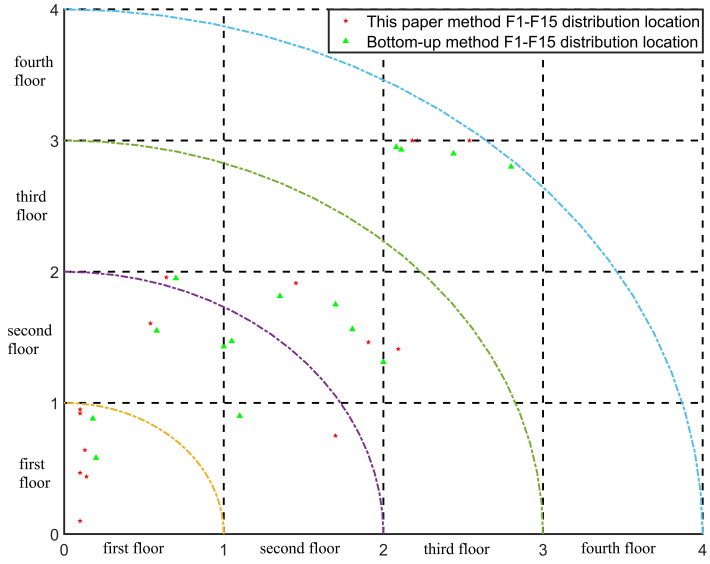

Figure 5. Distribution of link task likelihood hierarchy positions based on two methods.

aforementioned adjustments are reasonable when combined with the comprehensive risk prediction results calculated in this section.

Compared to the entropy method, the weight value of F_2 obtained using the proposed method is relatively low. The main reason is that the link task F_2 has higher value-at-risk when using the entropy method. If the information of the attacking entity is not fully understood, it will seriously hinder the total task execution and even cause a fatal blow. However, this paper argues that F_2 is very important. More importantly, we must allocate our forces and respond to physical attacks based on our knowledge of the enemy's posture when making comprehensive risk predictions. Therefore, it is reasonable that the combined weight of F_2 obtained by the proposed method is lower than that obtained using the entropy method.

In addition, compared to the scenario strain shortage capacity risk F_{12}, the impact of the unreasonable indicators system of program preference risk F_{13} on the overall program performance is relatively large, and the weight of F_{12} in F should be lower than the weight of F_{13} in F. Compared with the literature[40], it is more effectively reflected in the proposed method.

According to the risk weight value of each link task given by the defense expert system, the link task weight value obtained by each method in Table 10 is analyzed by using the Technique for Order of Preference by Similarity to Ideal Solution (TOPSIS) ideal point method[42–44], and the decision matrix[45] constructed is shown in Table 11, where the elements indicate the difference between the weights of each link task given by different methods and expert systems. Based on Table 11, the calculated TOPSIS evaluation results are shown in Table 12.

As can be seen from the results in Table 12, compared with the other two methods, the comprehensive score index of the method proposed in this paper is higher and is the optimal program, indicating that the risk weight value of each link of the task obtained by our technique is most consistent with the actual situation.

Table 9. The centrality of the link task risk

F_i	$C(F_i)$	F_i	$C(F_i)$	F_i	$C(F_i)$
F_1	0.4080	F_6	2.3650	F_{11}	0.6400
F_2	1.8120	F_7	2.0930	F_{12}	0.0000
F_3	1.1710	F_8	1.0000	F_{13}	0.4490
F_4	1.4500	F_9	2.0090	F_{14}	0.9200
F_5	1.2210	F_{10}	1.1470	F_{15}	0.4670

Table 10. Table of intra-tier weights for the link tasks

Weight judgment matrix $B_h = (b_{ij})_{g_h \times g_h}$							Methodology of this study			Bottom-up extraction method			Entropy method
							Levels	Intra-layer weights	Composite weights	Levels	Intra-layer weights	Composite weights	
F_8	1	2	2	2	2	2		0.3278	**0.0822**	2nd Floor	0.1713	**0.0443**	0.0480
F_{11}	0	1	2	2	0	2	1st Floor	0.1684	0.0422	1st Floor	0.7311	0.1887	0.0631
F_{12}	0	0	1	0	0	0		**0.0619**	**0.0156**	4th Floor	**0.1015**	**0.0262**	**0.0725**
F_{13}	0	0	2	1	0	0		**0.0864**	**0.0217**	2nd Floor	**0.0770**	**0.0199**	**0.0674**
F_{14}	0	2	2	2	1	2		0.2349	0.0589	1st Floor	0.2689	0.0694	0.0343
F_{15}	0	0	2	2	0	1		0.1206	**0.0303**	2nd Floor	0.1148	**0.0296**	0.0451
F_4	1	0	2				2nd Floor	0.2889	0.0822	3rd Floor	0.1674	0.0074	0.0842
F_9	2	1	2					0.5628	0.0422	2nd Floor	0.3813	0.1887	0.0654
F_{10}	0	0	1					0.1483	0.0589	2nd Floor	0.2556	0.0694	0.0535
F_5	1	0	0				3rd Floor	0.1483	0.0492	3rd Floor	0.1015	0.0236	0.0631
F_6	2	1	2					0.5628	0.1481		0.4551	0.0990	0.0720
F_7	2	0	1					0.2889	0.0339		0.2760	0.0719	0.0474
F_1	1	0	0				4th Floor	0.5627	**0.1315**	4th Floor	0.4551	**0.0310**	0.1244
F_2	2	1	2					**0.1484**	**0.0330**		0.1674	**0.0121**	**0.0642**
F_3	2	0	1					0.2889	**0.1701**		0.2760	**0.1188**	0.0954

Table 11. TOPSIS decision-making matrix

Segment task risk items	Methodology of this article	Bottom-up extraction method	Entropy method	Segment task risk items	Methodology of this article	Bottom-up extraction method	Entropy method
F_1	0.0015	0.099	0.081	F_9	0.0578	0.0887	0.0348
F_2	0.003	0.0179	0.0404	F_{10}	0.0089	0.0194	0.0135
F_3	0.0002	0.0515	0.0995	F_{11}	0.0578	0.0887	0.0288
F_4	0.0022	0.0726	0.0219	F_{12}	0.0026	0.0132	0.0701
F_5	0.0292	0.0036	0.0336	F_{13}	0.0044	0.0062	0.0605
F_6	0.0171	0.032	0.0762	F_{14}	0.0369	0.0474	0.0387
F_7	0.0039	0.0419	0.0472	F_{15}	0.0087	0.008	0.0442
F_8	0.0062	0.0317	0.006				

Table 12. TOPSIS evaluation results

Method	Positive ideal solution distance	Negative ideal solution distance	Composite score index	Arrange in order
Methodology of this article	**1.06422349**	**3.52206885**	**0.76795559**	1
Bottom-up extraction method	2.85681912	2.18487242	0.43336099	2
Entropy method	2.98084338	2.11787522	0.41537402	3

Combining the link task risk values in Table 2 and the link task weights in Table 10, the risk value of the total

Table 13. Comparison of integrated risk forecast results

	Actual combined risk value	Bottom-up extraction method	Entropy method	Methodology of this article
Comprehensive Risk	0.6621	0.6485	0.6764	0.6676

Table 14. Deviation between the predicted value of each integrated risk and the actual integrated risk value

	Bottom-up extraction method	Entropy method	Methodology of this article
Deviation	13.82%	15.83%	**6.08%**

task is obtained using Equation (15). The integrated risk value evaluated by the air defense expert system was taken as the actual integrated risk value, and was compared and analyzed with the risk values obtained by each of the aforementioned methods, as shown in Table 13.

Table 13 shows that the relative error rate between the integrated risk value obtained by the proposed method and the actual risk value is 0.82%, while the relative error rates of the other two approaches are 2.1% and 2.11%.

6.4. Comparative analysis of different methods

To further illustrate the overall advantages of the proposed method, the risk values of 20 test samples are predicted; the detection samples are obtained by collecting basic data of the defense side in exercise tasks in different scenarios. The real comprehensive risk values based on the expert system were 0.5327, 0.6745, 0.8871, 0.7125, 0.6265, 0.5292, 0.7715, 0.4858, 0.6142, 0.5383, 0.7627, 0.5475, 0.4965, 0.6057, 0.7322, 0.8447, 0.5737, 0.7124, 0.5325, and 0.6581. The risk values predicted by the proposed method, bottom-up extraction method, and fuzzy hierarchical analysis were compared. The validation outcomes illustrate the feasibility and reasonableness of the proposed method. The actual integrated risk values of the 20 test samples and the predicted integrated risk values obtained by different methods are shown in Figure 6. The deviation of each predicted value from the actual integrated risk value is calculated, as given in Table 14.

It can be seen from Table 14 that the deviation between the proposed method and the actual comprehensive risk value is minimal. Compared with bottom-up extraction, the relative deviation is reduced by 56%. Compared with the entropy weight method, the relative deviation is reduced by 61.6%. It shows that this method can predict the comprehensive risk of defense mission planning more accurately and exhibits certain feasibility.

7. CONCLUSION

In this paper, the relation between links and tasks is systematically expounded. On the premise of considering different association types, the hierarchy determination method of the link task in the whole defense task is explored. The decision graph of link task risk level for efficient defense task planning is generated. Then, a comprehensive risk prediction model is constructed. The problem of inaccurate risk prediction results caused by non-independence between tasks is solved. Through the simulation of test samples, the feasibility and rationality of the proposed method are compared and analyzed. The work and innovation of this paper are mainly reflected in:

(i) Defining the types of link inter-task associations as hierarchical, synergistic and independent relationships, further deepening the connotation of associative relationships, and proposing a calculation method for link tasks.

(ii) Introducing the idea of hierarchical topology, a method for determining the hierarchical position of link tasks based on rotational extraction is proposed, and the reasonableness of the generated hierarchical topology paths is analyzed based on the level of significance in the path analysis method.

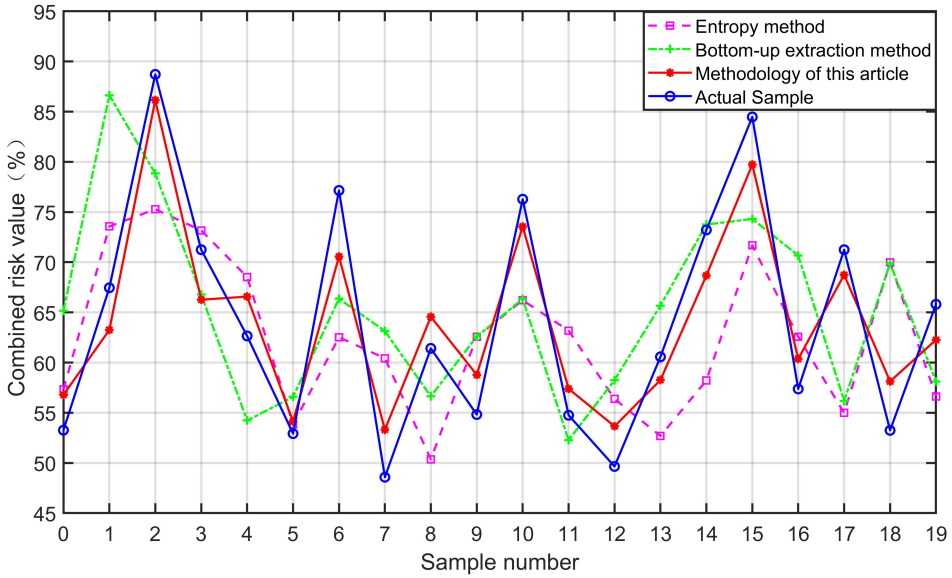

Figure 6. Comparative chart of integrated risk forecast results

(iii) A hierarchical decision weighted mapping of integrated risk is constructed using the link task centrality degree. Compared with the entropy weight method, this paper considers the correlation type and intensity of tasks in weight calculation. The result is more consistent with the actual situation, and the relative deviation of risk is reduced by 61.6%. Compared with the bottom-up extraction method, the nodes in the graph constructed in this paper are more centralized to the root node, and the relative risk deviation is reduced by 56%. To some extent, the proposed method solves the problem that the existing decision-making methods are difficult to reflect the correlation strength of link tasks, which leads to unreasonable prediction results.

In summary, the integrated risk prediction method for defense mission planning with hierarchical weighted mapping proposed in this paper shows significant advantages in dealing with the complex risk environment of planning missions in the field of national defense and can provide scientific decision support for strategic deployment. At the same time, the method can also be applied to risk decision-making in financial investment, emergency management, urban planning and construction. However, the construction of risk terms proposed in this paper is not comprehensive enough, and we will further improve the accuracy of comprehensive risk prediction by refining and expanding the risk terms in the future.

DECLARATIONS

Acknowledgments

The authors would like to thank the reviewers for their thoughtful comments and efforts towards improving this manuscript.

Authors' contributions

Methodology, experiment, data analysis, and manuscript drafting: Du W
Conceptualization, manuscript edition and review, and supervision: Chen X

Availability of data and materials

Not applicable.

Financial support and sponsorship
None.

Conflicts of interest
Both authors declared that there are no conflicts of interest.

Ethical approval and consent to participate
Not applicable.

Consent for publication
Not applicable.

REFERENCES

1. Gong J, Lu C, Liu Q, Huang J. Uncertain mission planning for earthquake rescue based on scenario. Proceedings of the 2022 IEEE 2nd international conference on electronic technology, communication and information (ICETCI), Changchun, China, 27-29 May 2022; pp. 586-92. DOI
2. Yue L, Yang R, Zhang Y, Yu LX, Wang Z. Deep reinforcement learning for UAV intelligent mission planning. *Complexity* 2022;2022:3551508. DOI
3. Kase SE, Hung CP, Krayzman T, Hare JZ, Rinderspacher BC, Su SM. The future of collaborative human-artificial intelligence decision-making for mission planning. *Front Psychol* 2022;13:850628. DOI
4. Xu J, Liu T, Tian W, Wang X, Zhang J, Chen Y. Safety risk assessment based on reloading airdrop mission. *E3S Web Conf* 2021;257:02084. DOI
5. Zhang Y, Zuo F. Selection of risk response actions considering risk dependency. *Kybernetes* 2016;45:1652-67. DOI
6. Dixit V. Risk assessment of different sourcing contract scenarios in project procurement. *Int J Constr Manag* 2022;22:1537-49. DOI
7. Lin SS, Shen SL, Zhou A, Xu YS. Risk assessment and management of excavation system based on fuzzy set theory and machine learning methods. *Automat Constr* 2021;122:103490. DOI
8. Li Y, Hu Z. A review of multi-attributes decision-making models for offshore oil and gas facilities decommissioning. *J Ocean Eng Sci* 2022;7:58-74.DOI
9. Duan L, He J, Li M, et al. Based on a decision tree model for exploring the risk factors of smartphone addiction among children and adolescents in China during the COVID-19 pandemic. *Front Psychiatry* 2021;12:652356. DOI
10. Wu J, Gong H, Liu F, Liu Y. Risk Assessment of open-pit slope based on large-scale group decision-making method considering non-cooperative behavior. *Int J Fuzzy Syst* 2023;1:245-63. DOI
11. Ikwan F, Sanders D, Hassan M. Safety evaluation of leak in a storage tank using fault tree analysis and risk matrix analysis. *J Loss Prevent Proc Ind* 2021;73:104597. DOI
12. Zheng HL, Du WW, Zhao XX, Shi H. Operational conception risk assessment model. *Fire Control Command Control* 2021;4:110-5;121. DOI
13. Song YB, He JL, Sun JZ, Xu T. Evaluation on joint operation determination scheme. *Command Inf Syst Technol* 2016;4:49-54. DOI
14. Ryczynski J, Tubis AA. Tactical risk assessment method for resilient fuel supply chains for a military peacekeeping operation. *Energies* 2021;14:4679. DOI
15. Kim I, Kim S, Kim H, Shin D. Mission-based cybersecurity test and evaluation of weapon systems in association with risk management framework. *Symmetry* 2022;14:2361. DOI
16. Zhang Y, Liu J, Xie X, Wang C, Bai L. Modeling of project portfolio risk evolution and response under the influence of interactions. *Mathematics* 2023;11:4091.DOI
17. Abedzadeh S, Roozbahani A, Heidari A. Risk assessment of water resources development plans using fuzzy fault tree analysis. *Water Resour Manag* 2020;34:2549-69. DOI
18. Du WW, Chen XW. Operational task hierarchical decomposition. *Acta Armamentarii* 2021;42:2771. DOI
19. Lei S, Peng XR, Li XS. Research on the evaluation of national defense science and technology strategic intelligence research capability based on QFD. *Inf Stud Theory Appl* 2022;2:55-60. DOI
20. Costa LF. Further generalizations of the Jaccard index. *arXiv* 2021. DOI
21. Zhang D, You X, Liu S, Yang K. Multi-colony ant colony optimization based on generalized jaccard similarity recommendation strategy. *IEEE Access* 2019;7:157303-17. DOI
22. Chung NC, Miasojedow B, Startek M, Gambin A. Jaccard/Tanimoto similarity test and estimation methods for biological presence-absence data. *BMC Bioinformatics* 2019;20:1-11. DOI

23. Hsu WK, Chen J, Huynh NT, Lin Y. Risk assessment of navigation safety for ferries. *J Mar Sci Eng* 2022;5:700. DOI
24. Yu Y, He X, Wan F, Bai Z, Fu C. Dynamic risk assessment of karst tunnel collapse based on fuzzy-AHP: a case study of the LianHuaShan tunnel, China. *Adv Civil Eng* 2022;2022:4426318. DOI
25. Li K, Xiahou X, Huang H, et al. AHP-FSE-Based risk assessment and mitigation for slurry balancing shield tunnel construction. *J Environ Public Health* 2022;2022:1666950. DOI
26. Fan C, Deng B, Yin Y. Hierarchical structure and transfer mechanism to assess the scheduling-related risk in construction of prefabricated buildings: an integrated ISM–MICMAC approach. *Eng Constr Archit Manag* 2023;30:2991-3013. DOI
27. Chen Y, Lou N, Liu G, Luan Y, Jiang H. Risk analysis of ship detention defects based on association rules. *Mar Policy* 2022;142:105123. DOI
28. Song W, Zhu Y, Li S, Wang L, Zhang H. Risk evaluation of information technology outsourcing project: an integrated approach considering risk interactions and hierarchies. *Eng Appl Artif Intell* 2022;113:104938. DOI
29. Wei DT, Liu XD, Guo R. Research on strategic consistency evaluation method of equipment system based on improved DEMATEL-ISM-FCA. *Military Oper Res Assess* 2021;3:29-35. DOI
30. Mathiyazhagan K, Govindan K, NoorulHaq A, Geng Y. An ISM approach for the barrier analysis in implementing green supply chain management. *J Clean Prod* 2023;47:283-297. DOI
31. Ajmera P, Jain V. A fuzzy interpretive structural modeling approach for evaluating the factors affecting lean implementation in Indian healthcare industry. *Int J Lean Six Sigma* 2019;2:376-97. DOI
32. Wang M, Zhang Y, Tian Y, Zhang K. An integrated rough-fuzzy WINGS-ISM method with an application in ASSCM. *Expert Syst Appl* 2023;212:118843. DOI
33. Amini A, Alimohammadlou M. Toward equation structural modeling: An integration of interpretive structural modeling and structural equation modeling. *J Manag Anal* 2021;4:693-714. DOI
34. Ahmad N, Qahmash A. Smartism: implementation and assessment of interpretive structural modeling. *Sustainability* 2021;16:8801. DOI
35. Niati DR, Siregar ZME, Prayoga Y. The effect of training on work performance and career development: the role of motivation as intervening variable. *BIRCI J* 2021;2:2385-93. DOI
36. Heri S, Nur AY, Mohd H, Rico NI, Irada S. Relationship between budget participation, job characteristics, emotional intelligence and work motivation as mediator variables to strengthening user power performance: an emperical evidence from indonesia government. *Morfai J* 2021;1:36-48. DOI
37. Hirdinis M. Capital structure and firm size on firm value moderated by profitability. *Int J Econ Business Admin* 2019;VII:174-91. DOI
38. Poduval PS, Pramod VR, Raj VPJ. Interpretive structural modeling (ISM) and its application in analyzing factors inhibiting implementation of total productive maintenance (TPM). *Int J Qual Reliab Manag* 2015;3:308-31. DOI
39. Sarabi S, Han Q, Romme AGL, de Vries B, Valkenburg R, den Ouden B. Uptake and implementation of nature-based solutions: an analysis of barriers using interpretive structuralmodeling. *J Environ Manag* 2020;270:110749. DOI
40. Sharma A, Abbas H, Siddiqui MQ. Modelling the inhibitors of cold supply chain using fuzzy interpretive structural modeling and fuzzy MICMAC analysis. *Plos One* 2021;16:e0249046. DOI
41. Zhu Y, Tian D, Yan F. Effectiveness of entropy weight method in decision-making. *Math Problems Eng* 2020;2020:3564835. DOI
42. Nor-Al-Din SM, Razali NK, Sukri NM, Rosli MA. Application of TOPSIS method for decision making in selecting the best new car in Malaysia. *IOP Conf Ser Mater Sci Eng* 2021;1176:012040. DOI
43. Chakraborty S. TOPSIS and modified TOPSIS: a comparative analysis. *Decis Anal J* 2022;2:100021. DOI
44. Siregar VMM, Sonang S, Purba AT, Sugara H, Siagian NF. Implementation of TOPSIS algorithm for selection of prominent student class. *J Phys Conf Ser* 2021;1783:012038. DOI
45. Watrobski J, Baczkiewicz A, Ziemba E, Sałabun W. Sustainable cities and communities assessment using the DARIA-TOPSIS method. *Sustain Cities Soc* 2022;83:103926. DOI